DOI: 10.1515/FAS-2017-0012
FATIGUE OF AIRCRAFT STRUCTURES (2017)
S. 157–170

EXPERIMENTAL AND NUMERICAL STUDY OF NACA AND CONVENTIONAL RIVETING PROCEDURE

Wojciech Wronicz, Jerzy Kaniowski, Maciej Malicki, Paweł Kucio and Robert Klewicki[1]

Institute of Aviation, Poland

Abstract

Fatigue behaviour is one of the most important properties of modern airplanes and rivets influence it strongly. According to the literature, the NACA riveting offers a multiple increase in the fatigue life of joints.

The aim of this paper is to investigate the benefits offered by the NACA riveting procedure with respect to the residual stress and strain distribution after riveting as well as rivet hole expansion. Experimental and numerical approaches were adopted. The conventional riveting with both the universal and countersunk rivets was compared with the NACA riveting. The countersunk angle and depth in the case of the NACA riveting was modified somewhat relative to the values met in the literature. For these three cases, strain gauge measurements during riveting, hole expansion measurements and FE calculations were performed. The hole expansion measurement with the use of Computer Tomography(CT) was proposed.

Only the FE calculations unambiguously indicate better fatigue properties of the NACA riveting. The proposed method of hole expansion measurement requires further research to increase its accuracy.

Keywords: rivet, NACA riveting, fatigue, hole expansion, computed tomography.

1. INTRODUCTION

Fatigue behaviour is one of the most important properties of modern airplanes as it determines the service life of a structure as well as necessary inspections and their frequency. These affect strongly an aircraft's direct operating cost. In metal airframes, rivets are usually of critical importance from the fatigue point of view since cracks usually nucleate near them. At the same time, the fatigue life of riveted joints is influenced strongly by a riveting technology and can vary over twenty times for the same specimen and loads, depending on the riveting technology used.

In 1997, at the ICAF symposium, Müller and Hart-Smith presented the paper *Making Fuselage Riveted Lap Splices with 200-year Crack-Free Fatigue Lives* [1]. They investigated the fatigue life of the 3-row countersunk-rivet lap splices and obtained a 25-fold increase in fatigue life (compared to the fatigue life of splices riveted with the minimum allowable force) with the use of a high riveting force and the NACA riveting method. Despite such promising results, there are only very few articles devoted to the fatigue properties of the NACA riveting. Figure 1. illustrates this method. The authors believe that this method is worth investigating with the use of capabilities offered by contemporary technology.

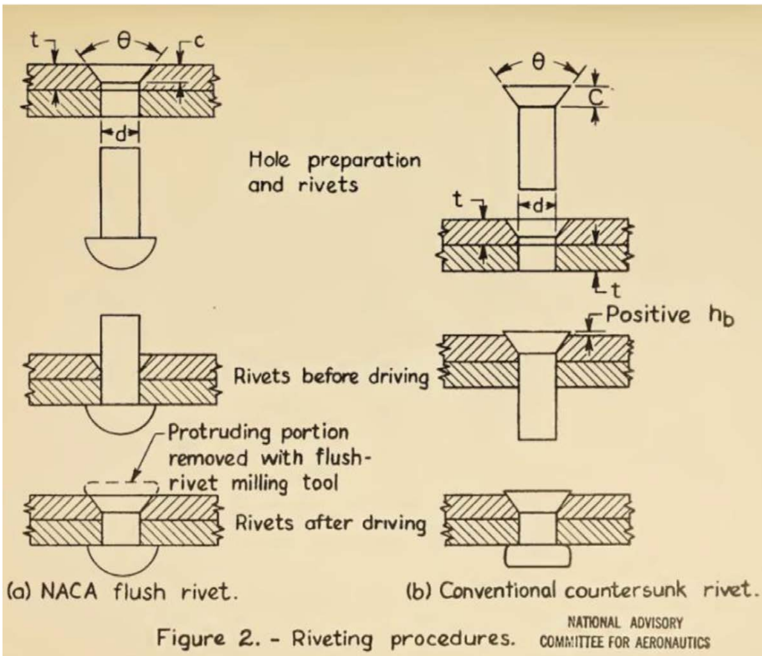

Figure 1. NACA and conventional riveting [2]

It is commonly accepted that the stress system around a rivet is decisive for the crack nucleation and propagation. This stress system results from external loads and residual stresses, induced mainly during riveting. In some cases, it is possible to obtain around the rivet compressive radial and tangential residual stresses that delay crack initiation and growth [3], [4]. Residual stresses after riveting can be also estimated by the hole expansion and this parameter can be used to assess the quality of a joint [3]. Fatigue cracks typically start on the faying surface and this area is particularly important.

The aim of this paper is to investigate the benefits offered by the NACA riveting procedure with respect to the residual stress and strain distribution after riveting. Experimental and numerical approaches were adopted. The conventional riveting with both the universal and countersunk rivets was compared with the NACA riveting. For these three cases, strain gauge measurements during riveting, hole expansion measurements and FE calculations were performed. The hole expansion was measured with the use of Computed Tomography (CT).

2. STRAIN GAUGE MEASUREMENTS

2.1.Experiment

Strain progress during riveting was recorded with the use of strain gauges on the specimens shown in Figure 2. Each specimen consisted of two bare sheet made of 2024-T3 alloy with the nominal thickness equal to 1.6 mm. The geometry of the specimens was designed as a two row lap joint with six rivets to allow using the specimens for fatigue tests in the future.

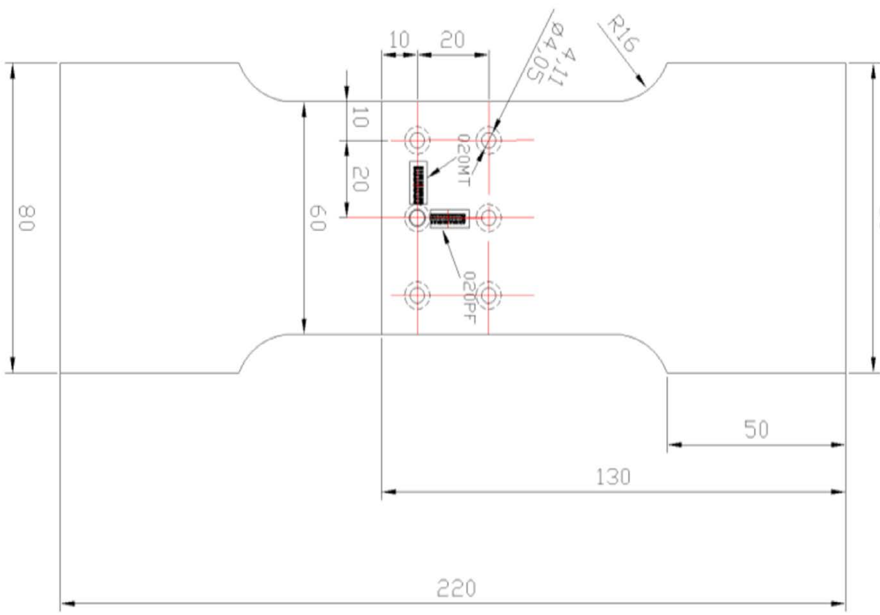

Figure 2. Geometry of specimens for strain gauge measurements

Three specimens for each of the three configurations (conventional riveting with a both universal and countersunk rivet and the NACA riveting) were prepared. Rivets made of 2117 alloy with a diameter equal to 4 mm were used in all cases. In the case of conventional riveting, MS20470AD5-5 and NAS1097AD5-5 (rivet length 7.9 mm) rivets in T4 condition were used. For the NACA riveting, MS20470AD5-6 rivets in T0 condition (rivet length 9.5 mm, annealed) were selected. During the first tests, rivets in standard T4 conditions were used for the NACA riveting. Because of the problem with the filling of the countersunk by the driven head, the rivets were annealed, frozen and riveted in soft T0 condition.

The lack of detailed technological information poses considerable difficulty in investigating the NACA riveting. Based on [56] and information obtained via emails from Dr L.J. Hart-Smith (author of [1, 5-6]) and from Mr Johannes Homan from the Fatec Engineering as well as FE calculations, the following assumptions were made: rivet length 9.5 mm, standard countersunk angle 90° (instead of 82°), countersunk depth 1,6 mm (whole sheet thickness) and diameter of the driven head equal to 1.8 times the rivet shank diameter. According to the information from Dr L.J. Hart-Smith, such change in the countersunk angle does not affect the joint performance substantially while the deeper countersunk results in higher fatigue life.

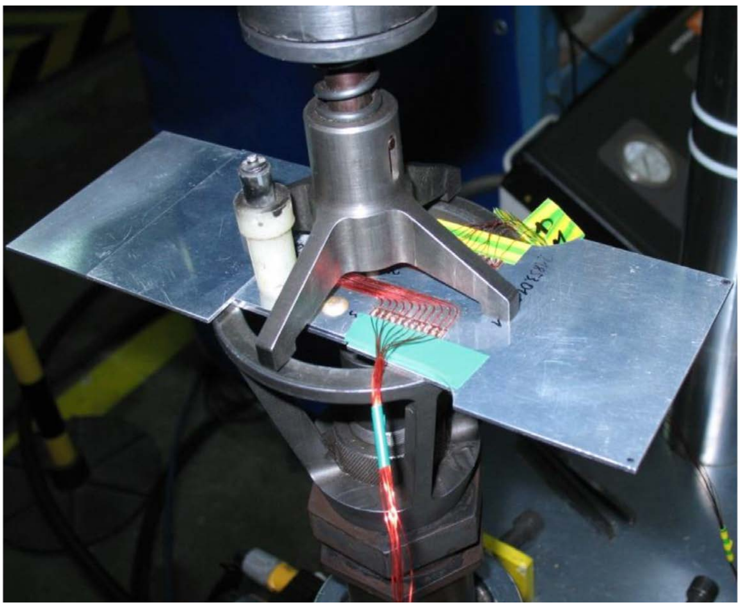

Figure 3. Specimen during riveting

On the sheet surface near the central rivet hole, on the driven head side, the strip strain gauges were applied. Vishay strip gauge patterns type 020MT and 020PF with gauge length of each section equal to 0.51 mm were selected due to a high strain gradient near the rivet. At first, outer rivets were installed, then radial (020MT) and tangential (020PF) strains were recorded during squeezing the central rivet. The riveting force level was selected experimentally before tests to obtain the driven head diameter 1.8 times and 1.7 times greater than the rivet shank diameter for the NACA and the conventional riveting respectively. These values were equal to 25 kN for the universal rivet, 27 kN for the NACA riveting and 24.5 kN for the countersunk rivet. A special riveting device (Figure 3.), developed for the purposes of the previous investigation [4], was used to avoid damaging the strain gauges. Force controlled riveting was performed with the MTS 312/68 testing machine, and strains were recorded in half-bridge configuration with the National Instruments CompacRIO system.

2.2. Results

Strains were recorded on three specimens for each configuration. The position of each strain gauge was measured with the optical microscope and the graphs of strains as the function of the distance from the rivet axis were prepared. To make results more clear, average strains for each configuration were calculated. Because there were small differences in gauges location, the linear interpolation was used to determine strains for selected positions. In the case of evidently incorrect result (damage of a particular section), the result was not taken into account. Figure 4. shows average radial and tangential strains for the investigated configurations as the function of distance from the rivet axis divided by the rivet shank radius. The highest strains (tensile and compressive) were recorded for the NACA riveting, the lowest for the universal rivets.

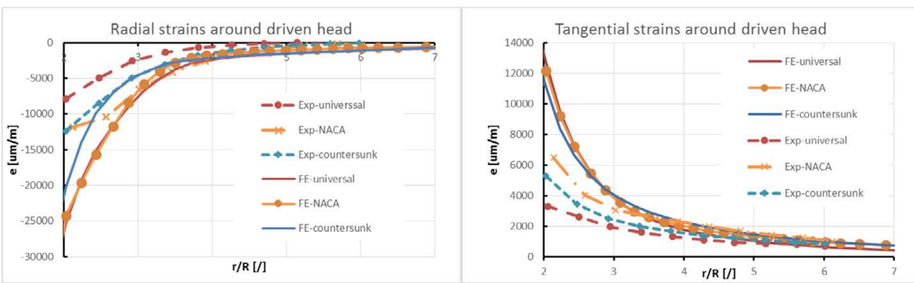

Figure 4. Average strains near driven head for investigated configurations

3. FINITE ELEMENT CALCULATIONS

Residual stress distribution on the faying surface is critical from the fatigue point of view. Unfortunately, this region is inaccessible for the experimental method except the neutron diffraction [7,8]. The Finite Element Method enables the investigation of this area. Numerical models should be validated and verified with the experiment, where measurements are possible to ensure compliance with reality.

3.1. Model

The Finite Element axisymmetric models were prepared to analyse the three cases described above. The quasistatic riveting process was simulated with a nonlinear implicit algorithm (MSC MARC). Each model consisted of deformable (sheets and the rivet) and rigid (tools) contact bodies and about 2500 linear elements and 2700 nodes. During the analysis, all rigid curves did not move except for the stamp, which moved down squeezing the rivet shank until it reached the appropriate force level. Then, the force was gradually released.

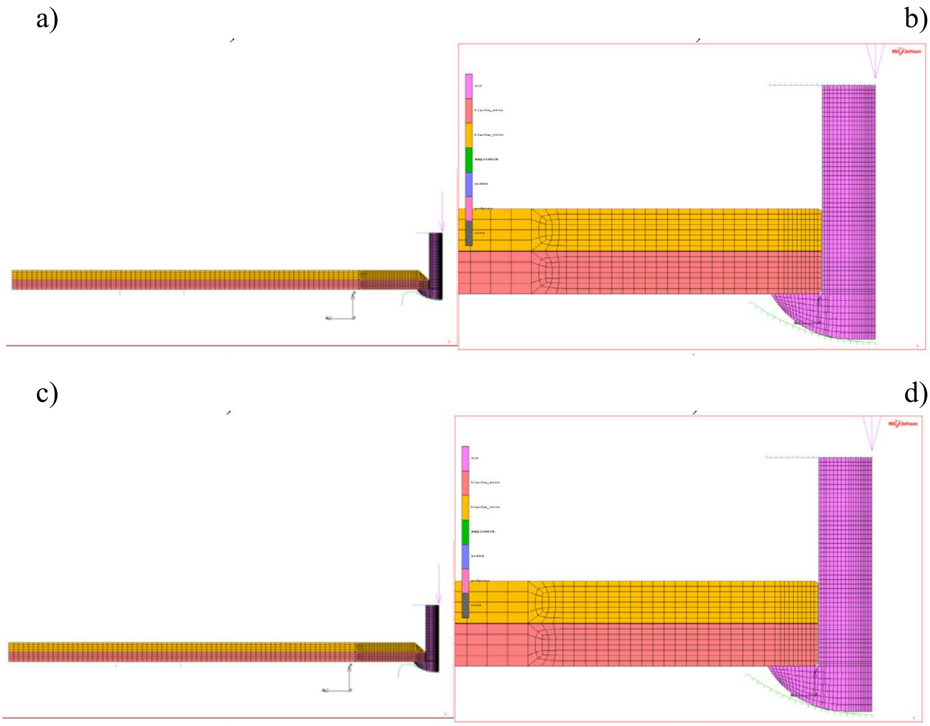

Fig. 5. FE models, a) entire model, central part of: b) universal rivet model, c) NACA rivet model, d) countersunk rivet model

The material models were developed based on the monotonic tests. In the case of rivets in T0 (soft) condition, riveting with one sheet was performed and a force-displacement curve for the stamp was recorded. The same conditions were simulated numerically. Then, the model of 2117-T4 alloy was modified in such a way that a good correlation with the experimental force-displacement curve for the stamp was achieved (Figure 7). Stress-strain curves of the material models used in FE analyses were presented in Figure 6.

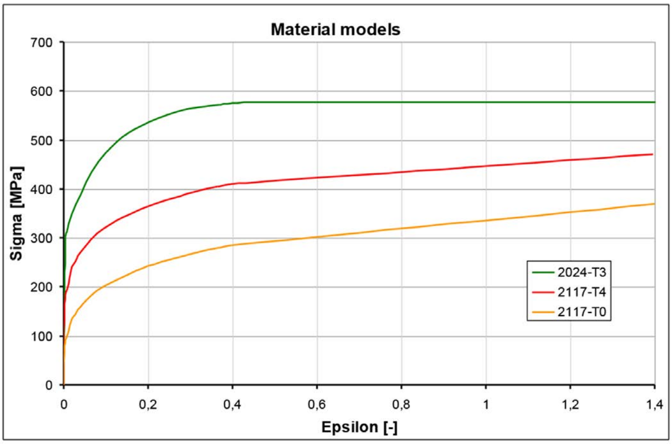

Fig. 6. Material models used in FE analyses

3.2. Experimental verification

At first, the force-displacement curves for the press stamp obtained experimentally and in calculation were compared for the purpose of installing a universal rivet in one sheet. Two heat treatments, T4 and T0 were analysed (Figure 7).

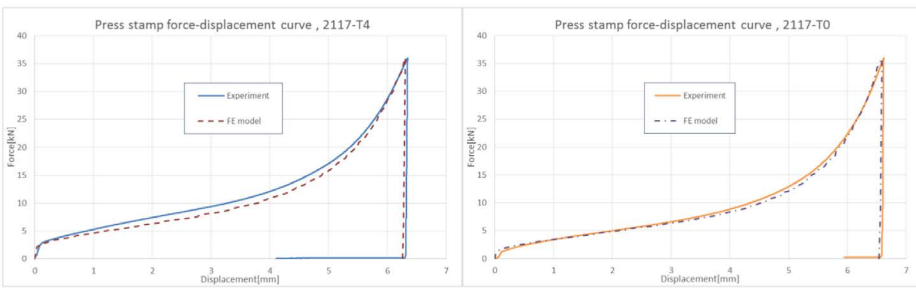

Fig. 7. Comparison of FE and experimental stamp force-displacement curves

Then, the riveting simulation of the three cases for which strains were recorded, was performed. Numerical results were compared with measured strains (average for the particular case). Figure 8. shows radial and tangential strains near the driven head. Good correlation of radial strains was obtained in the case of the countersunk rivet and the NACA riveting. In the case of the universal rivet, strains obtained numerically were substantially higher than measured values. In the case of tangential strains, numerical results were overestimated close to the rivet and were almost the same for the three cases. Also, it should be noted that the differences between experimental curves were negligible and that each of these curves represented average values for three specimens.

The FE models of the universal and countersunk rivets differed in the geometry and slightly in the force level (according to the experiment), but correlation with measured values was significantly better for the countersunk rivet. For experiment, these rivets were provided by various suppliers and could differ slightly in material properties or heat treatment. This problem did not exist in calculations.

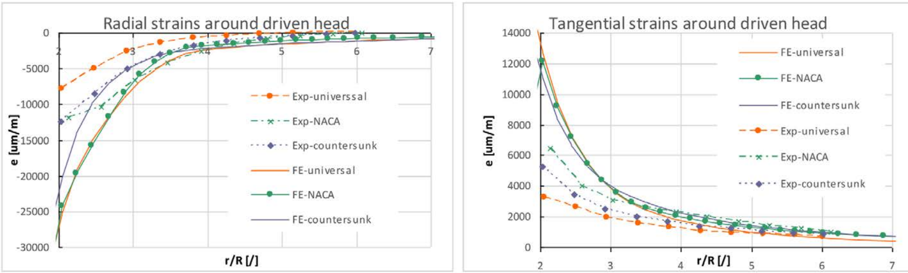

Fig. 8. Comparison of strains near driven head obtained in experiment and numerically

3.3. Results

From the fatigue point of view, the most critical location is the faying surface since cracks typically nucleate in this region. Figure 9. presents stress courses on the faying surface for both sheets. The most beneficial stress distribution was obtained for the NACA riveting. The maximum of the tensile stresses (tangential) are the lowest and it was placed the furthest from the rivet axis. In the external sheet, the universal rivet gave somewhat lower tensile stresses, but its maximum was closer to the rivet. Moreover, the NACA riveting provided the longest range, where tangential stresses were compressive. Also, radial compressive stresses were the highest in this case but differences were smaller here. For the same reasons, the universal rivet offered the worst stress distribution in the internal sheet, when the countersunk rivet in the external sheet.

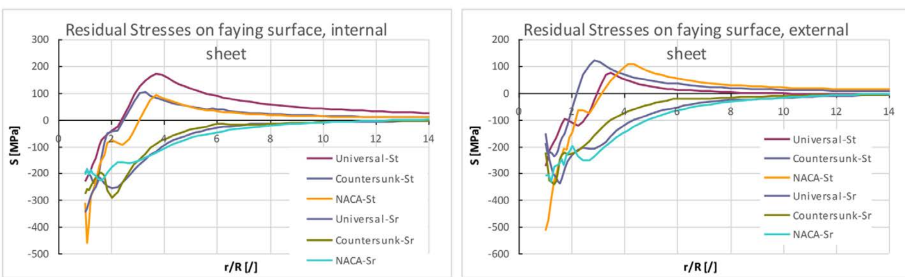

Fig. 9. Residual stress courses on faying surfaces, Sr-radial stresses, St-tangential stresses

4. RIVET HOLE EXPANSION MEASUREMENTS

Rivet hole expansion (h_e) is defined as an increase in a rivet hole diameter expressed as a percentage of an initial hole diameter ($h_e = [(d_e - d_0)/d_0]*100\%$, where d_e and d_0 is the initial and expanded rivet hole diameter respectively). This parameter indicates a degree of sheets cold working during riveting and residual stresses level which are directly associated with the rivet expansion.

Rivet hole expansion is usually measured by destructive methods. Müller [3] has proposed two such methods. One involves cutting the rivet with sheets near to the rivet axis (perpendicularly to sheets) and then sanding and measuring the cross section until the rivet axis is reached. Then, the rivet diameter can be measured at any desired level along sheets thickness. The disadvantage of this approach is that residual stresses are partially released and that the exact determination of the rivet axis position (which affects values measured) is not obvious. The other method involves extracting the rivet by sawing sheets from two sides. After separation, rivet diameter can be measured at a desired level. All residual stresses induced by the rivet-sheet interference were released and elastic spring back occurred. According to Müller, this effect is not significant as results he obtained with these two methods were very similar. The second method offered a lower scatter.

Skorupa et al. [9] have proposed another method. At first, both rivet heads are cut away, then sheets with the rivet shank are consecutively removed by milling (parallel to sheets) to a desired level (depth) and polished to facilitate measurements. The cross section is perpendicular to the rivet axis what eliminates the problem of determination its position. Moreover, this method definitely does not influence the stress state of the joint as much as the above described approaches do. The disadvantage is that measuring at the next level requires that the material be removed so it is impossible to re-measure diameter at the previous level.

The author has proposed to use Computed Tomography (CT) to determine the rivet hole expansion. Compared to the procedures used in [3] and [9], this method is non-destructive and enables measuring the diameter without releasing any residual stresses and eliminates necessity of having the subsequent layers removed. The possibility of measuring the diameter at many more layers in the thickness direction is also an advantage. The disadvantage of this method is lower accuracy compared to direct optical measurements.

4.1. Experiment

Specimens shown in Figure 10. were prepared for the measurements of the rivet hole expansion with the use of Computed Tomography. For the three cases for which strain measurements were performed, joints were manufactured with the same configuration (rivet type, diameter, length and material, squeezing force). Then, each joint was scanned on the GE Phoenix v|tome|x s 240 CT scanner with the same specimen position (the same scale).

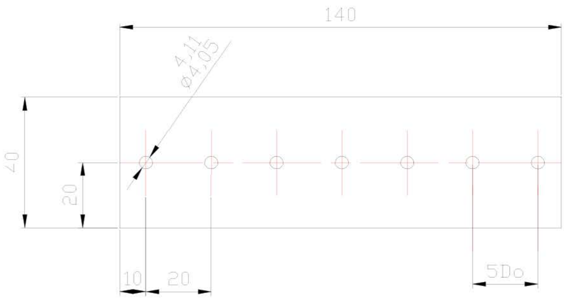

Fig. 10. Specimen geometry used in rivet hole expansion measurements

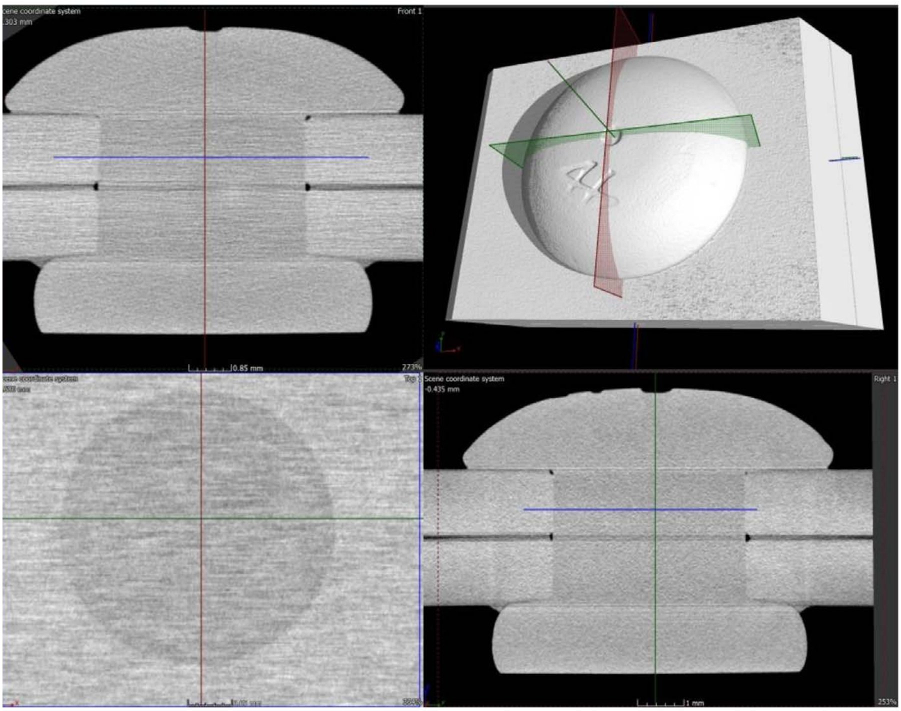

Fig. 11. Examples of Computed Tomography scan of rivet

The VG Studio MAX and MyVGL software were used for geometry processing (reconstruction) and generation of CT images across sheet thickness. After reconstruction, the coordinate system axes were aligned with the rivet axis and specimens edges. Figure 11. presents an image of a joint and three sections. Then, CT images for sheets surfaces and multiple levels through sheets thickness were prepared end exported to the DraftSight software (JPEG format). A distance measurement was marked on each image for scaling. Anadditional scale correction, the same for all images, was introduced based on measurements of the driven head diameters, since it was not performed during scanning. On each image of the cross section (perpendicular to the rivet axis), a circle was drawn based on selected three points to best fit it to the rivet shank boundary and the diameter of this circle was measured. This method facilitates the determination of the rivet shank diameter in the case of not distinct boundary on a part of an image. The accuracy of such fitting was estimated to be about 0,02 mm based on the scatter of diameters determined several times on the same images. The initial hole diameters were assumed based on the measurements made prior to riveting.

CT scanning provided some additional observations. The chamfer at the hole edges were not completely filled by the rivet shank during riveting, except the chamfers under the driven head. A crevice between the driven head and the sheet was filled with some material, probably clad, which was pushed during riveting. The inner sheet was squeezed under the driven head and had a smaller thickness in this area.

4.2. Results

Figure 12. shows the graph of hole expansion determined based on CT scans as a function of normalised position (distance from the inner sheet face divided by the sheet thickness). The '0' corresponds to the face of the internal sheet, the '1' to the faying surface and the '2' to the face of the external sheet. It should be noted that, in the case of the NACA riveting, the driven head is on the external sheet side, when for the other rivets, on the internal sheet side. The obtained results are similar for all types of rivets. A somewhat higher expansion obtained for the countersunk rivet could be a result of some differences in material characteristics. The hole expansion on the internal sheet is at a similar level for all series despite that, in the case of the NACA riveting, there is a manufactured head on this side, when for other rivets, a driven head. Generally, the hole expansion is higher on the driven head side, which is a benefit of the NACA riveting. In the case of the universal rivet, the lowest values of the hole expansion is near the manufactured head. The values of hole expansion are similar to the results presented in [3], but in current investigation, in the case of the countersunk rivet, there is not significant variation in the expansion across the thickness.

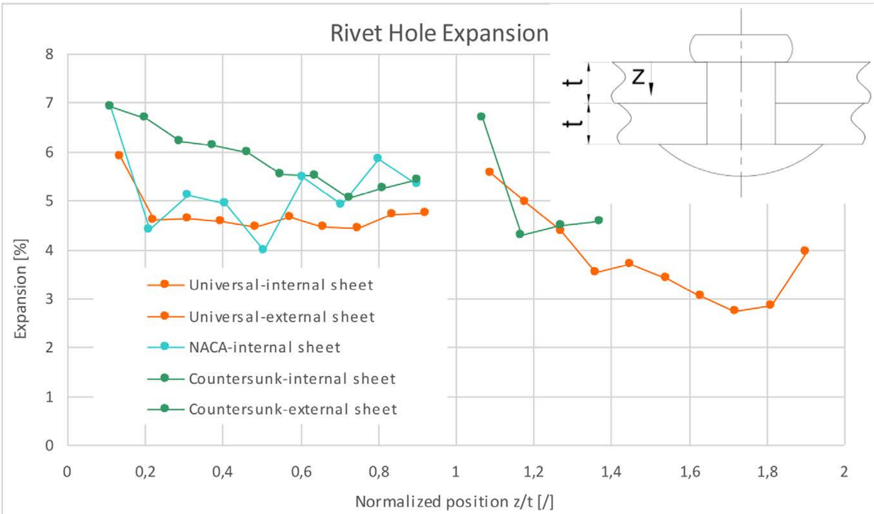

Fig. 12. Rivets hole expansion measured based on CT scans

5. CONCLUSIONS

According to the literature, the NACA riveting offers a huge increase in fatigue life of riveted joints. The aim of this paper was to investigate the benefits offered by this method with respect to the residual stress and strain distribution after riveting as well as to the rivet hole expansion. These data were determined and compared for the NACA riveting as well as for the conventional riveting with the use of the universal rivet and the countersunk rivet.

Strain measurements around driven heads showed that, from the fatigue point of view, the most beneficial residual strain distribution was obtained for the universal head rivet in the case of tangential strains (the lowest tensile strains) and for the NACA riveting in the case of radial strains (the highest compressive strains). For the countersunk rivet, the recorded strains were between values obtained for the other cases. Based on these data it is difficult to indicate which configuration will result in the highest fatigue life of joints.

To analyse the residual stress distribution on the faying surface, which is critical from the fatigue point of view, FE calculations were performed for the cases investigated experimentally. With respect to the forcedisplacement curve of the stamp, a very good correlation with the experiment was obtained. Residual strains near the driven head obtained numerically agreed with measured values quite well in the case of radial direction, especially for the countersunk rivet and the NACA riveting. For tangential strains, a correlation was worst. The difference in correspondence with the experiment between the universal and countersunk rivets could arise from slight material differences between these rivets. The results of the FE calculations indicate that the NACA riveting provides the best residual stresses on the faying surface.

The author has proposed to measure rivet hole expansion with the use of Computed Tomography. This method is non-destructive and enables measurements at multiple levels (depths). The highest values of expansion were obtained for the countersunk rivet, which can be associated with some material differences. The hole expansion on the internal sheet in the case of the universal rivet and the NACA riveting was at the same level despite that, in the case of the NACA riveting, there was a manufactured head on this side, when for the other rivets, a driven head. Generally, hole expansion was higher on a driven head side, which indicates a beneficial characteristics of the NACA riveting. The use of Computed Tomography to determine rivet diameter at multiple levels was possible thanks to different material (alloy) of the rivet and sheet, since, in the case of a properly installed rivet, there was not a slit between a rivet shank and sheets. The method needs further investigations to increase its accuracy and the verification with traditional destructive methods.

So far, only the FE calculations have unambiguously indicated better fatigue properties of the NACA riveting. However, any conclusive evaluation will have to involve fatigue tests, which are planned in the future. It should be also noted that the countersunk angle and depth in the NACA riveting differ somewhat from the values met in the literature and possible impact of these differences requires additional analysis.

6. ACKNOWLEDGEMENT

The author would like to express his gratitude to Dr L.J. Hart-Smith and Mr Johannes Homan for their kindness and valuable information.

The researches were financed from the subsidy granted by the Polish Ministry of Science and Higher Education for statutory activities of the Institute of Aviation.

The paper was presented during the 29th ICAF Symposium in Nagoya, 7–9 June 2017.

REFERENCES

[1] R. P. G. Müller and L. J. Hart-Smith. (1997). *Making fuselage riveted lap splices with 200-year crack-free-lives*, in Proceedings of the 19th ICAF Symposium, Fatigue in New and Aging Aircraft, Edinburgh, Scotland, pp. 18–20.

[2] M. Mandel and L. Bartone. (1944). *Tensile Tests of NACA and Conventional Machine-Countersunk Flush Rivets*, NACA, Langley Memorial Aeronautical Laboratory, Advance Restricted Report L4F06.

[3] R. P. G. Müller. (1995). *An experimental and analytical investigation on the fatigue behaviour of fuselage riveted lap joints*. PhD Dissertation, TU Delft, Delft University of Technology.

[4] W. Wronicz and J. Kaniowski. (2011). *Experimental and Numerical Study of Strain Progress During and After Riveting Process for Brazier Rivet and Rivet with Compensator - Squeezing Force and Rivet Type Effect*, Fatigue Aircr. Struct., vol. 2011, no. 3, pp. 166–190.

[5] L. J. Hart-Smith. (2003). *Forgotten Attributes of NACA Rivet Installations and Ice-Box Rivets*, in Proceedings of the 7th Joint FAA/DoD/NASA Aging Aircraft Conference, New Orleans, Louisiana.

[6] L. J. Hart-Smith. (2010). *Lessons Learned by One Aerospace Structures Engineer in a 40-Year Career*, in Proceedings of the 6th Australasian Congress on Applied Mechanics, ACAM 6, Perth, Australia. pp. 12–15.

[7] C. Rans, P. V. Straznicky and R. Alderliesten. (2007). *Riveting process induced residual stresses around solid rivets in mechanical joints*. J. Aircr., vol. 44, no. 1, pp. 323–329.

[8] G. Li, G. Shi, and N. C. Bellinger. (2004). *Neutron diffraction measurement and FE simulation of residual strains and stress in fuselage lap joints*, Institute for Aerospace Research, National Research Council of Canada, LTR-SMPL-2004-0003.

[9]

M. Skorupa, A. Skorupa, T. Machniewicz, and A. Korbel. (2010). *Effect of production variables on the fatigue behaviour of riveted lap joints*, Int. J. Fatigue, vol. 32, no. 7, pp. 996–1003.